Photothermal Inhibition of Neural Activity with Near-Infrared-Sensitive Nanotransducers

Sangjin Yoo,[†] Soonwoo Hong,[⊥] Yeonho Choi,[⊥] Ji-Ho Park,[†,‡,§,*] and Yoonkey Nam[†,§,*]

[†]Department of Bio and Brain Engineering, [‡]KAIST Institute for Optical Science and Technology, [§]KAIST Institute for the NanoCentury, Korea Advanced Institute of Science and Technology (KAIST), 291 Daehak-ro, Yuseong-gu, Daejeon 305-701, Republic of Korea and [⊥]Department of Biomedical Engineering, College of Health Science, Korea University, Jeongneung 3-dong, Seongbuk-gu, Seoul 136-703, Republic of Korea

ABSTRACT A neural stimulation technique that can inhibit neural activity reversibly and directly without genetic modification is valuable for understating complex brain functions and treating brain diseases. Here, we propose a near-infrared (NIR)-activatable nanoplasmonic technique that can inhibit the electrical activity of neurons by utilizing gold nanorods (GNRs) as photothermal transducers on cellular membranes. The GNRs were bound onto the plasma membrane of neurons and irradiated with NIR light to induce GNR-mediated photothermal heating near the membrane. The electrical activity from the cultured neuronal networks pretreated with GNRs was immediately inhibited upon NIR irradiation, and fully restored when NIR light was removed. The degree of inhibition could be precisely modulated by tuning the laser intensity, thereby enabling restoration of firing of a hyperactive neuronal network with epileptiform activity. This nanotechnological approach to inhibit neural activity provides a powerful therapeutic platform to control cellular functions associated with disordered neural circuits.

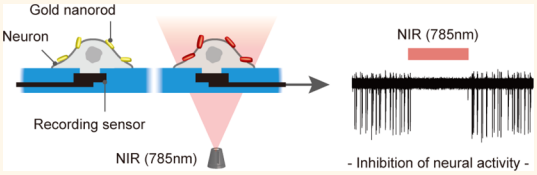

KEYWORDS: epileptic seizure · gold nanorod · neuromodulation · photostimulation · photothermal therapy

Nanomaterials have attracted a great deal of attention in the field of cellular engineering as their physicochemical properties can be utilized to precisely modulate cellular signaling pathways and behaviors. For example, nanomagnetic actuation and heating with iron-based nanoparticles have been used to remotely control the functions and behaviors of intracellular molecules.[1−4] Photoactive heating with carbon-based nanomaterials facilitated selective regulation of gene expression in the intracellular region.[5] Despite their great potential in the field of cellular engineering, little effort has focused on engineering functional nanomaterials for modulation of neural functions associated with brain disorders.

Electrical and chemical stimulation have been widely used to modulate neural activities in the nervous system. Electrical stimulation is mainly intended to excite nerve tissues by depolarizing membrane potentials, while chemical stimulation can be used for both excitation and inhibition by modulating synaptic transmission. However, it is difficult to utilize these methods for selective and precise control of cellular activity due to the limited spatial or temporal resolution.[5,6] Optical stimulation methods have been introduced to enhance sptaiotemporal resolution. Direct irradiation with infrared light has been shown to affect the excitability of nerve cells by generating thermal gradients surrounding the nerve tissues.[7−10] Optogenetics, which combines optical stimulation with genetic modification of target cells, has been used to selectively stimulate a subpopulation of neurons in neural tissues.[11,12] Although optogenetic methods enabled researchers to control excitation and inhibition of neural activity with high cellular specificity, strong photocurrent for inhibitory opsins, stable gene expression, and NIR excitation of opsins for deep tissue penetration have yet to be achieved. In addition, the imperative genetic modification step for cell targeting impedes immediate clinical translation.[13] Therefore, it would be beneficial to develop a nongenetic optical stimulation technique that can modulate neural activity with deeper tissue penetration capabilities.

* Address correspondence to jihopark@kaist.ac.kr, ynam@kaist.ac.kr.

Received for review April 14, 2014 and accepted July 21, 2014.

Published online July 21, 2014
10.1021/nn5020775

To achieve improved inhibitory optical stimulation that does not require genetic modification, we attempted to affect neural excitability with photothermal capability of NIR sensitive GNRs. Recently, gold nanomaterials have emerged as biocompatible nanophototransducers for efficient conversion of optical radiation into localized heat in biological systems.[14] Gold nanorods have attracted particular interest for biological applications due to their strong absorption in the NIR region, where living tissues are relatively transparent. Localized heating mediated by GNRs upon NIR irradiation has been applied extensively for remote and selective destruction of malignant cells for cancer therapy;[15−17] however, there has been little effort to utilize GNRs for precise control of neural activity through the nanoscale photothermal effects. On the basis of our preliminary results on thermal suppression of neural activity in cultured neurons,[18] we hypothesized that efficient photothermal conversion mediated by GNRs bound on the neural membrane would enable the spatiotemporal suppression of neural activity. Here, we present a new neuromodulation technique that utilizes GNRs as photothermal nanotransducers on neural membranes to temporarily suppress or continuously modulate the activity of primary neurons from rat brain tissues (Figure 1A). GNRs were bound to the plasma membrane with minimal cellular uptake and exposed to continuous NIR laser irradiation to activate them for neural modulation. We found that GNR-mediated photothermal heating on the plasma membrane enabled the modulation of action potentials from cultured hippocampal neurons with external NIR light. In addition, we demonstrated that neural network activity was successfully restored in an *in vitro* epilepsy model using this photothermal modulation technique.

RESULTS AND DISCUSSION

We first engineered bare GNRs to bind on the neuronal plasma membrane. Cetyltrimethylammonium bromide (CTAB)-coated GNRs with longitudinal plasmon resonance at 785 nm were prepared using a previously established procedure.[19] The CTAB capping molecules on the GNR surface were replaced with positively charged amine-terminated polyethylene glycol (NH_2-PEG) to improve their biocompatibility and facilitate their binding to the negatively charged plasma membrane *via* electrostatic interactions. In transmission electron microscopy (TEM), bare GNRs were seen with axial sizes of 18.5 and 71.3 nm and a PEG coating of 3 nm (Figure 1B). PEGylation did not cause a spectral shift in plasmon resonance (Figure 1C). Terminal amine groups of the PEG coating rendered a positive charge on the surface of the GNRs (+ 21.3 mV, Figure 1D). Biocompatibility of GNRs on hippocampal neurons was significantly improved within the incubation period (up to 72 h) by PEGylation (Figure 1E). Furthermore, we examined whether the photothermal effect of PEGylated GNRs could be modulated by the NIR laser power by measuring the temperature change of the GNR solution. The photothermal effect increased with laser power (Figure 1F), indicating that the degree of photothermal heating applied to the neurons could be precisely modulated by the laser power. The surface modification of GNRs with amine-terminated PEG molecules led to their localization on the plasma membrane. Hippocampal neurons were isolated from prenatal rat brains, plated on cell culture plates, and treated with fluorescently tagged PEGylated GNRs for 9 h (Figure S1, Supporting Information). Confocal fluorescent microscopy clearly showed that most of the GNRs were localized on the plasma membrane (Figure 1G). Furthermore, the amount of GNRs bound on the membrane was quantified as a function of incubation time using their intrinsic multiphoton luminescence (Figure S2, Supporting Information).[20] The amount of GNRs bound on the membrane increased with increasing incubation time (Figure 1H).

We next investigated whether the local photothermal effect of GNRs attached to the plasma membrane was able to modulate spontaneous neuronal activity. Hippocampal neuronal networks were cultured on a multichannel microelectrode array (MEA) chip and incubated with GNRs. At specific time points (1, 3, 6, and 9 h postincubation), the neurons were repeatedly irradiated with a NIR laser (785 nm) (Figure 2A). The unbound GNRs remained in the medium during the irradiation. The medium temperature upon each irradiation was estimated to increase up to approximately 4−5 °C because of the unbound GNRs in the medium (Figure S3, Supporting Information). During the experiments, extracellular spikes of the neuronal network were recorded simultaneously from 59 microelectrodes of the MEA chip. NIR irradiation or GNR treatment alone did not affect the spontaneous activity of neurons (Figure 2B and Figure S4, Supporting Information). In the case of neurons pretreated with GNRs, fewer spikes were detected upon irradiation with the NIR laser. As the incubation time increased from 1 to 9 h, almost no spikes were detected during NIR irradiation (Figure 2C). Quantitative measurement of the changes in spike rates revealed that the degree of inhibition, which was measured by the decrease in spike rate, was increased with increasing GNR incubation time (Figure 2D). Compared to the control group that was not treated with GNRs (incubation time 0 h in Figure 2D, value: 0.48%), the GNR treated groups showed significant decreases in spike rates upon NIR irradiation. The neural activity was suppressed to 20% of the original level by NIR irradiation after 9 h treatment with 10 μg/mL of GNRs. Importantly, the neural inhibition occurred within less than 1 s after NIR irradiation (Figure S5, Supporting Information). Taken together with Figure 1H, theses observations indicated

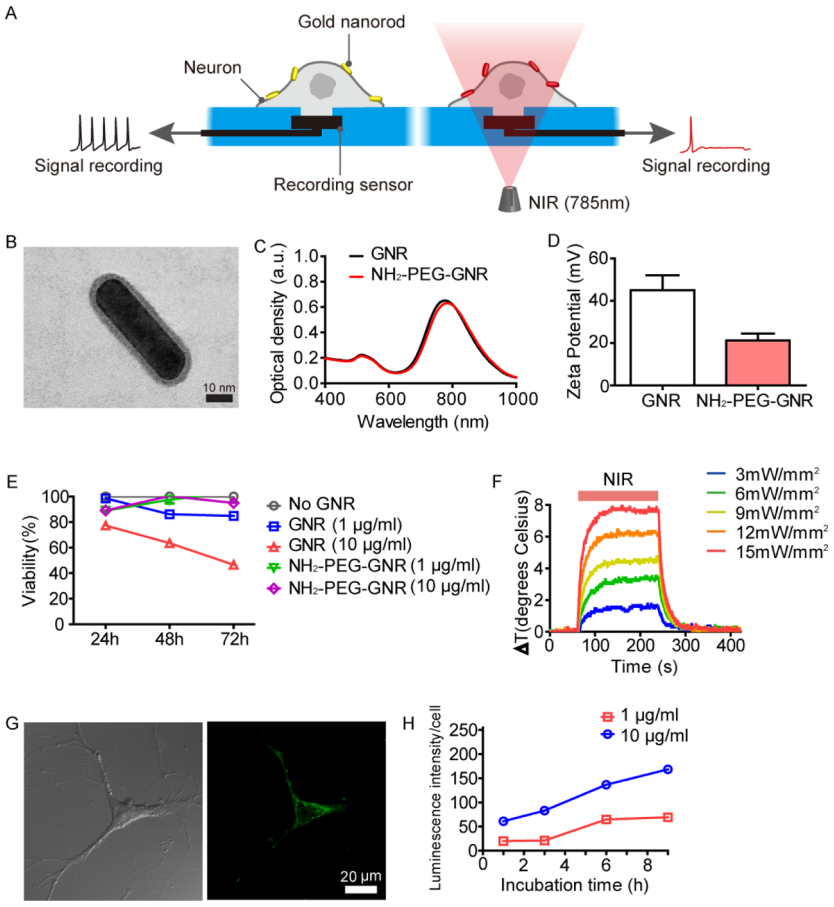

Figure 1. Gold nanorods and their interaction with neurons. (A) Schematic of gold-nanorod (GNR)-mediated photothermal stimulation of neurons. NH_2-terminated PEGylated GNRs (NH_2-PEG-GNR) localized on the neuronal membrane suppress neural activity through photothermal conversion of NIR energy. Changes in neural activities were recorded by extracellular electrodes. (B) TEM image of NH_2-PEG-GNR following treatment with phosphotungstic acid negative stain. The brighter region is associated with the PEG coating. (C) Absorption spectra of bare GNRs and NH_2-PEG-GNRs. (D) Zeta potential measurements of bare GNRs and NH_2-PEG-GNRs. (E) Cell viability of neurons treated with bare GNRs or NH_2-PEG-GNRs. The PEG coating of bare GNRs significantly improved their cell viability (Two way ANOVA followed by Bonferroni post hoc test; $p > 0.05$ for No GNR and 10 μg/mL NH_2-PEG-GNRs, $n = 50$ for each point). (F) Temperature changes in a solution of 10 μg/mL NH_2-PEG-GNRs at different laser power densities. Time constants (τ) of temperature rise and decay were 13.8 and 12.4 s, respectively. (G) Bright field (left) and fluorescence (right) images of neurons treated with fluorescently labeled NH_2-PEG-GNRs. (H) Quantification of NH_2-PEG-GNRs attached to the neurons with their intrinsic multiphoton-induced luminescence. (One way ANOVA, 1 μg/mL; $p < 0.0001$, 10 μg/mL; $p < 0.0001$, $n = 50$ for each point). All values represent mean ± SEM.

that more GNRs furthered the effect. Next, the degree of suppression was investigated with varying laser power density. As the laser power increased from 0 to 15 mW/mm^2, the degree of suppression increased monotonically from 0 to 89.6% (Figure 2E,F). Considering the temperature change and laser power (Figure 1F), this indicated that higher temperature further increased the suppression of neural activity. The temperature change on the GNR-bound membrane upon photothermal stimulation was estimated to understand the physiological conditions responsible for instant control of neural activity. Both numerical simulation and fluorescence measurement results revealed that the temperature on the membrane contacted directly with GNRs increases more rapidly and higher upon photothermal stimulation (~Δ8.5 °C within 800 ns in the simulation, Figure S6, Supporting Information; ~Δ10.5 °C within 10 s in the fluorescence measurement, Figure S7, Supporting Information), compared with the medium heating induced by the unbound GNRs (Δ4−5 °C within 10 s, Figure S3, Supporting Information). It suggests that the local GNR-mediated photothermal heating on the membrane contributes primarily to the instant inhibition of neural activity.

We next investigated the feasibility of GNR-mediated photothermal stimulation for long-term neural inhibition. Hippocampal neuronal networks were stimulated with intermittent NIR irradiation that last for a few minutes to several tens of minutes after 9-h incubation with GNRs. The results clearly demonstrated the capability of long-term inhibition of neural network (Figure 2G), which was demonstrated previously by an optogenetic technique using halorhodopsin.[21] There were no noticeable side effects of long-term photothermal stimulation as there were no significant

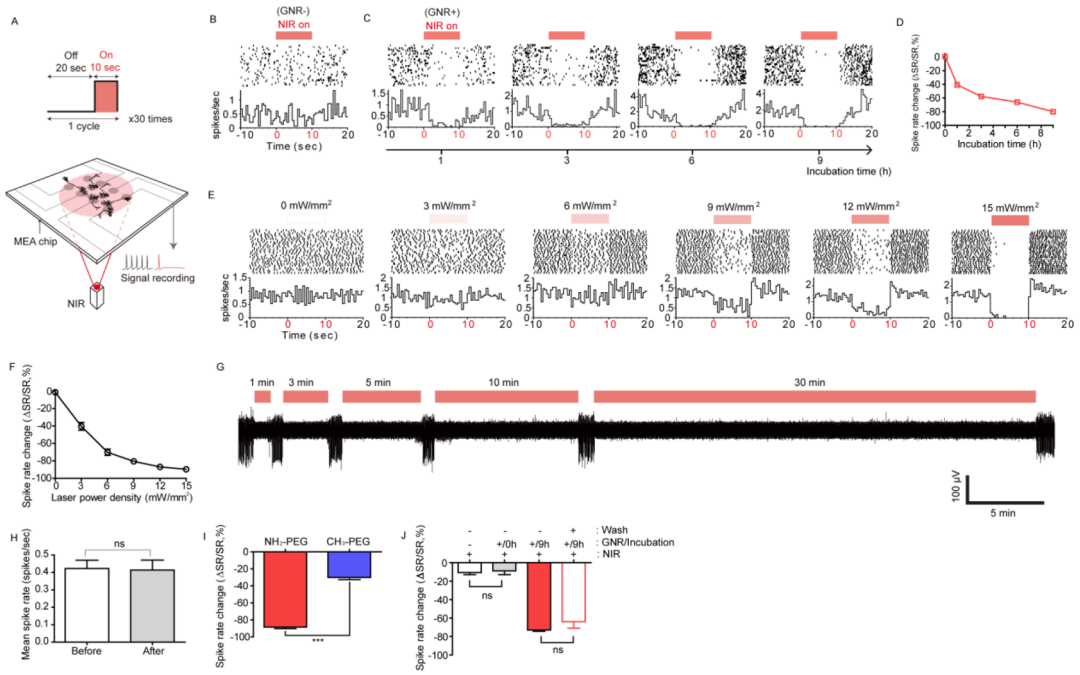

Figure 2. Photothermal modulation of spontaneous neural activity. (A) Schematic of repeated GNR-mediated photothermal stimulation of a neuronal network. Neurons were treated with NH_2-PEG-GNRs (10 μg/mL) and then repeatedly irradiated with a NIR laser (785 nm, 0−15 mW/mm^2). (B) Spike rates of untreated neurons upon repeated NIR irradiation (15 mW/mm^2). (C) Spike rates of neurons treated with NH_2-PEG-GNRs for different incubation times with NIR irradiation (15 mW/mm^2). (D) Quantification of spike rate changes of GNR-treated neurons upon repeated NIR irradiations in (C). One way ANOVA; $p < 0.0001$, $n = 264$ (0 h), 74 (1 h), 97 (3 h), 99 (6 h), 98 (9 h). The data point for $t = 0$ corresponds to no GNR treatment, as shown in (B). (E) Peri-event histograms and raster plots for different laser power densities. GNR incubation: 9 h. (F) Quantification of spike rate changes in (E). One way ANOVA; $p < 0.0001$, $n = 53$ (0 mW/mm^2), 54 (3 mW/mm^2), 54 (6 mW/mm^2), 54 (9 mW/mm^2), 58 (12 mW/mm^2), 58 (15 mW/mm^2). (G) A single trace of spike recording for different NIR irradiation periods (GNR incubation: 9 h, laser power density: 15 mW/mm^2). (H) Mean spike rates of GNR-treated neurons before and after NIR irradiation (Data were collected from the channels in which neuron activities were completely suppressed during NIR irradiation, two-tailed unpaired t test; $p = 0.9064$, $n = 40$ for each bar). (I) Changes in spike rates of neurons treated with NH_2- or CH_3-terminated PEGylated GNRs upon repeated NIR irradiation (Two tailed unpaired t test; $p < 0.0001$, $n = 105$ (NH_2) or 54 (CH_3)). (J) Changes in spike rates of neurons upon repeated NIR irradiation immediately after adding GNRs (0-h incubation) and neurons after 9-h incubation with GNRs followed by washing the unbound GNRs (wash) (Two-tailed paired t test; $p = 0.2296$ for NIR only ($n = 149$) and GNR/0 h ($n = 122$); $p = 0.5299$ for GNR/9 h ($n = 133$) and GNR/9 h + GNR washout ($n = 17$). The representative data in B, C, and E were recorded from different MEAs. Y-axis are not normalized. All values represent mean ± SEM.

differences in spike rates and spike shapes before and after suppression (Figure 2H and Figure S8, Supporting Information). Finally, the importance of the binding affinity of GNRs to the plasma membrane was examined by comparing the suppression between positively charged GNRs (NH_2-PEG-GNR, zeta-potential = 21.3 ± 13.5 mV, n = 17) and negatively charged GNRs (CH_3-PEG-GNR, zeta-potential = −35.5 ± 18.1 mV, n = 12). The surface of bare GNRs was modified with negatively charged methoxy-terminated PEG (CH_3-PEG) to reduce the binding affinity of GNRs to the plasma membrane (Figure S9, Supporting Information). In this case, the suppression was considerably weaker than that with positively charged amine-terminated GNRs (NH_2-PEG, Figure 2I), which suggested that the surface charge of GNR was important and sufficient numbers of membrane-bound GNRs were required for the inhibitory effect. We further investigated whether the GNRs bound on the membrane were responsible for the neuronal inhibition. Hippocampal neuronal networks were irradiated immediately after adding GNRs, and 9 h after incubation with GNRs followed by washing the unbound GNRs. These experiments exhibited that the GNRs suspended in the medium prior to binding to the membrane did not influence the neuronal activity significantly upon photothermal stimulation, whereas the GNRs bound directly to the membrane contributed primarily to the neuronal silencing (Figure 2J). Taken together, these results demonstrated that GNR-mediated photothermal stimulation could be utilized to precisely modulate suppression of cultured neuronal networks.

We investigated the effects of photothermal stimulation on electrically evoked neuronal activities by delivering short electrical pulses to cultured neurons. When electric current pulses are passed through a microelectrode, they produce action potentials from nearby neurons, which in turn spread throughout the neuronal network. In the MEA chip, we could focally stimulate the network by applying biphasic current pulses through a microelectrode and record neural responses by detecting spikes from neighboring

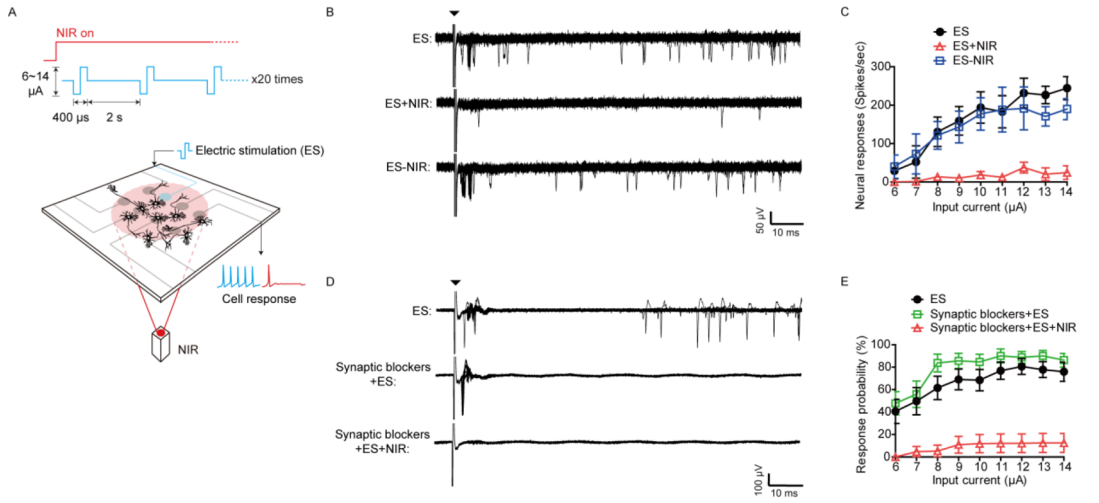

Figure 3. Photothermal modulation of electrically evoked neural activity. (A) Schematic of GNR-mediated photothermal stimulation of an electrically evoked neuronal network. Neurons were treated with NH_2-PEG-GNRs (10 μg/mL) for 9 h and evoked with repeated electrical stimulations (ES) with or without NIR irradiation (15 mW/mm^2). (B) MEA recordings following the electrical stimulation with or without NIR irradiations (20 overlapped traces, current level: 14 μA). (C) Quantification of spike rates of GNR-treated neurons upon NIR irradiation simultaneously with repeated electrical stimulations at different input current levels (Two way ANOVA; $p = 0.9109$ for ES and ES-NIR, $p < 0.0001$ for ES and ES+NIR, $n = 16$ for each point). (D) MEA recordings of electrically evoked GNR-treated neurons upon NIR irradiation after synaptic blockade. Current level: 14 μA, synaptic blocker: AP5 and CNQX (10 μM for each). (E) Quantification of neural responses with synaptic blockade (Two way ANOVA; $p = 0.0021$ for ES and Synaptic blockers+ES, $p > 0.0001$ for ES and Synaptic blockers+ES+NIR, $n = 16$ for each point). All values represent mean ± SEM.

microelectrodes (Figure 3A). Two types of responses were mixed in the recording: axonally conducted responses ("direct responses") and synapse mediated responses. Neural responses linearly increased with increasing input current over the range 6−14 μA (Figure 3B,C; ES). The neural responses evoked by electrical pulses were significantly suppressed upon photothermal stimulation (Figure 3B,C; ES+NIR). Importantly, the neural responses returned to the normal level once the photothermal stimulation was removed (Figure 3B, C; ES-NIR).

We next examined the effects of photothermal stimulation on a cell that was directly stimulated by the current pulses. To isolate these "direct" responses from synapse mediated responses, postsynaptic excitatory receptors such as AMPA and NMDA receptors were pharmacologically blocked by CNQX and AP5, respectively.[22] After synaptic blockade, electrically evoked neural activity only appeared within a 10 ms poststimulation window, indicating that the neural responses were collected primarily from the neurons that were directly stimulated by electrical current pulses (Figure 3D,E; ES). In addition, the response probability was slightly increased and the response latency was reduced after synaptic blockade, which was consistent with a previous report (Figure 3D,E; Synaptic blockers+ES).[22] The direct neural response was also significantly suppressed by photothermal stimulation (Figure 3D,E; Synaptic blockers+ES+NIR). The suppression of evoked responses under synaptic blockade indicated that the photothermal stimulation directly interfered with the generation of action potentials. In the control experiments, NIR irradiation without GNR pretreatment did not affect electrically evoked neural activity and physiological features of the neurons (Figure S10, Supporting Information).

We further examined whether the GNR-based suppression effect could be used as a neuromodulation technique to control the hyperexcited neural activity that is frequently observed in abnormal neural tissues with epilepsy. The experiment was performed by inducing hyperexcited activity in a cultured neuronal network, which was followed by controlling the intensity of photothermal stimulation to restore the original network activity level (Figure 4A). Epileptiform neural activity was induced by treating the cultured neuronal networks with bicuculline (BCC), which disinhibited the network by blocking the inhibitory synapses.[23−25] The results are shown in raster plots of nine units detected from MEAs and the mean firing rate histogram (Figure 4A,B). After treatment with BCC, there was a 2-fold increase in mean spike rate in the network, which was maintained for 8 min. The intensity of photothermal stimulation was manually adjusted from the maximum value (15 mW/mm^2) and set to the point where the mean spike rate was similar to the normal state. When the NIR laser was turned off to remove the external control, the neural activity returned immediately to its hyperexcited state. These observation indicated that the neural suppression can be utilized to achieve precise neuromodulation of hyperactive neural tissues using closed-loop negative feedback control.

Finally, we investigated how GNR-mediated photothermal heating influenced neuronal activity.

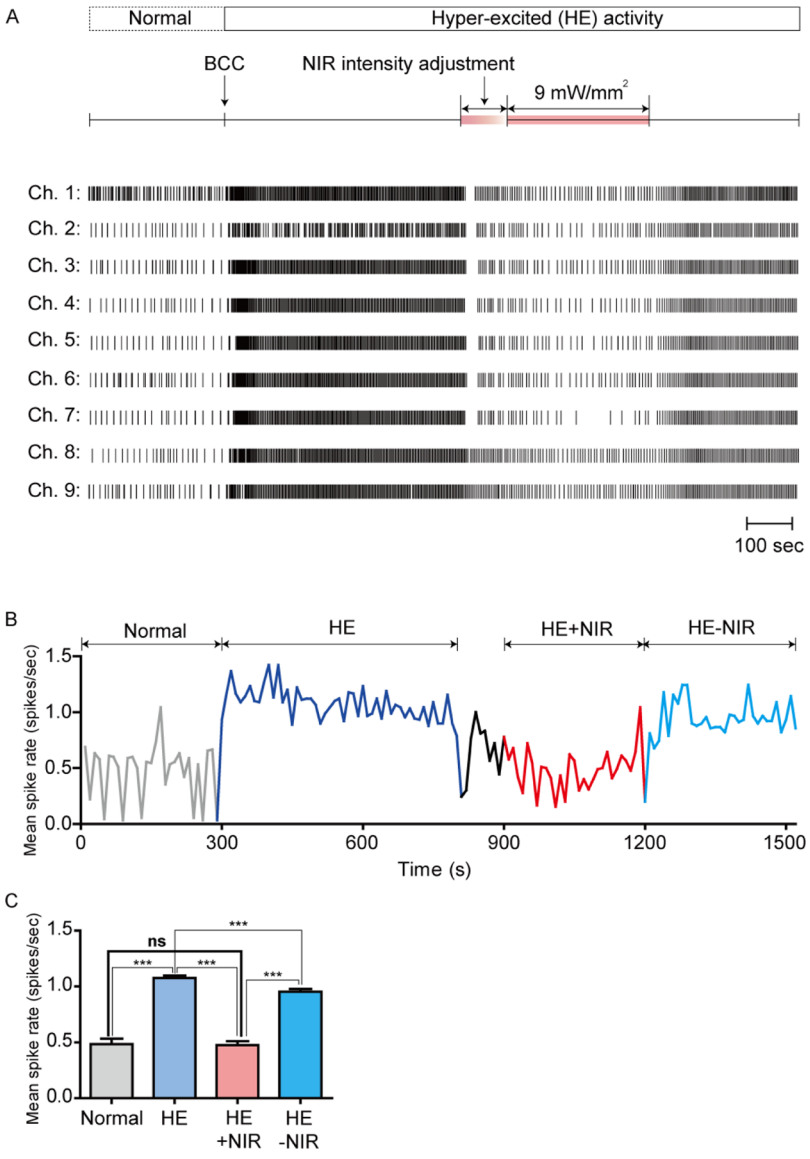

Figure 4. Photothermal modulation of epileptiform neural activity. (A) Firing activities of hyperexcited neurons upon photothermal stimulation. GNR-treated neurons (10 μg/mL, 9 h) were hyperexcited by bath application of bicuculline (BCC, 15 μM) and the laser power density was adjusted for restoration of neural activity (9 mW/mm^2). Signals of neural activity at multiple channels were simultaneously recorded during photothermal modulation on an extracellular neurosensor chip. (B) Mean spike rates of hyperexcited GNR-treated neurons upon NIR irradiation in (A). (C) Quantification of mean spike rates of hyperexcited GNR-treated neurons upon NIR irradiation (Two-tailed unpaired *t* test, ***p < 0.0001, n = 9 for each point). All values represent mean ± SEM.

We hypothesized that the heat delivered onto neuronal plasma membrane by GNRs could be responsible for the instant suppression of neural activity by delivering nanoscale heating to thermosensitive ion channels. First, we compared the suppression induced by macroscale heating with that of GNR-mediated nanoscale photothermal heating. For macroscale heating, a heating plate installed beneath the MEA chip was ramped to 41.5 °C at a rate of 0.054 °C/s (Figure 5A). The suppression of neural activity was observed when the medium temperature reached close to 40 °C and the effect disappeared gradually once the heat was removed (Figure 5B). These observations also confirmed that heat delivery was the main mechanism underlying the suppression. Comparing the time course of suppression, the GNR-mediated photothermal stimulation enabled instant suppression and recovery of neural activity, while heater-mediated stimulation took several minutes due to the longer response time for heat transfer from the heating plate to the cell through the glass chip and media (Figure 5B,C). These results clearly showed that nanoscale thermal effects had tremendous advantages over macroscale heating for the precise temporal control of neural activity. We also examined which ion channels are responsive to heat, leading to the suppression of action potentials in hippocampal neurons. One candidate was the TREK-1 channel (thermosensitive potassium channel),

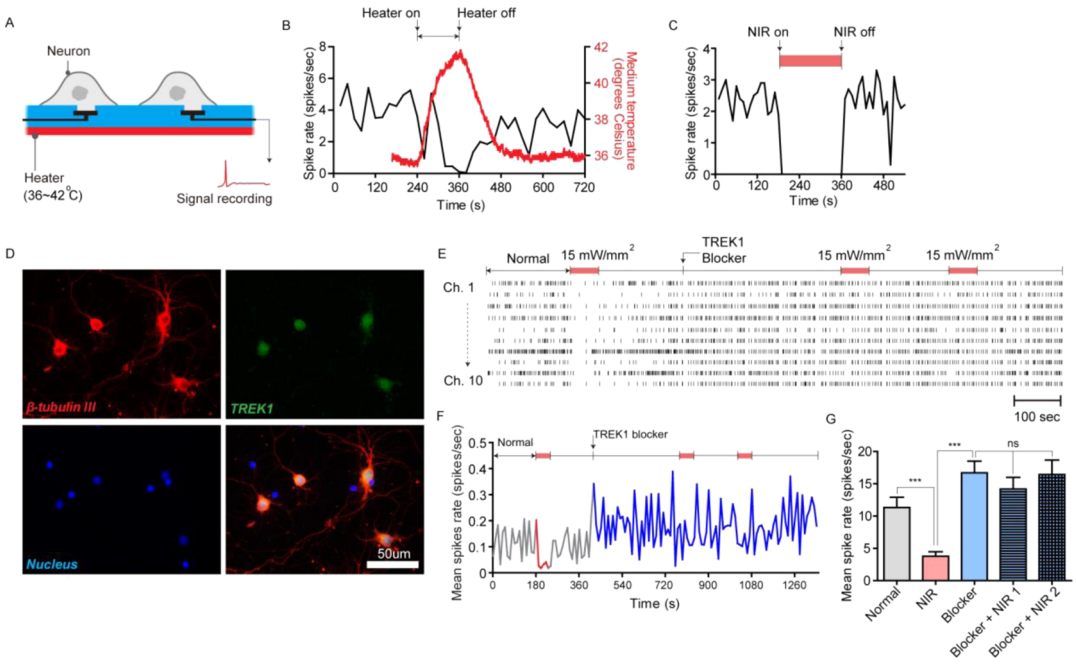

Figure 5. Nanoscale thermal effects on neural activity. (A) Schematic of a heating system to induce bulk thermal effects on neuronal network. (B) Neuronal spike rates and medium temperature upon thermal stimulation with bulk heating system. (C) Spike rates of neurons stimulated by GNR-mediated photothermal heating (10 μg/mL, 9 h, 15 mW/mm^2). (D) Fluorescence images of neurons after immunochemical staining for β-tubulin(III) (red), TREK-1 (green), and nucleus (blue). (E) Firing activities of GNR-treated neurons upon NIR irradiation after blocking TREK-1 channels. GNR-treated neurons were treated with fluoxetine (TREK-1 blocker, 1 μM) and then repeatedly irradiated for photothermal stimulation (10 μg/mL, 9 h, 15 mW/mm^2). (F) Mean spike rates of GNR-treated neurons upon NIR irradiation after blocking of TREK-1 channels in (E). (G) Quantification of mean spike rates of GNR-treated neurons upon NIR irradiation after blocking of TREK-1 channels. (Two-tailed unpaired *t* test, ***$p < 0.0001$, $n = 10$ for each point). All values represent mean $\pm$ SEM.

which was reported to be widely expressed throughout the entire brain region including the hippocampus and to intrinsically reduce neural activity.[26−28] Figure 5D shows immunolabeling of TREK-1 channels, which verified expression of these ion channels in the cultured hippocampal neurons used in this study. To verify the involvement of TREK-1 channels in the suppression, GNR-mediated photothermal stimulation was carried out with and without the TREK-1 channel blocker fluoxetine.[29,30] Figures 5E,F show raster plots and spike rate histograms for the experiment, respectively. When TREK-1 was blocked, the existing suppression disappeared (Figure 5G), which strongly suggested that TREK-1 channels are intimately involved in the neurothermal suppression induced by GNR and NIR irradiation.

In this study, we found photothermal inhibition of action potentials using membrane-bound NIR-activatable nanotransducers. The combination of NIR light and nanotransducer has advantages over other optical methods to modulate neural activity. In optogenetics, light-driven pumps such as halorhodopsin or archaerhodopsin must be genetically expressed by viral delivery to suppress neural activity.[12,21,31,32] The technique presented here obviates the need for genetic modification and enables deeper tissue penetration with NIR light. In direct NIR or IR laser stimulation methods, photothermal heating mainly led to the increase of neuronal activity,[7−10] which was opposite to our results. This discrepancy may come from different experimental parameters used in each study such as cell type, laser wavelength and intensity, and baseline temperature to cause different neural response mechanisms. In addition, a recent study demonstrated the transient and selective suppression of neural activity with pulsed IR laser stimulation,[33] which was in good agreement with what we observed in this study. Overall, our approach shows an excellent example of optical stimulation combined with exogenously introduced nanomaterials.

The main mechanism of the photothermal inhibition has yet to be determined. However, our results strongly suggest that the TREK-1 channel, which is known to be a thermosensitive potassium channel, is involved in the inhibition of action potentials through membrane-localized photothermal effects (Figure 5). Previous studies reported that the TREK-1 channel is expressed in the whole brain,[27,34] indicating that the suppression effect by photothermal stimulation would not be limited to hippocampal neurons. Indeed, the neurothermal suppression was also observed in cultured neurons from the cortex and olfactory bulbs (Figure S11, Supporting Information). The expression of TREK-1 channels in various types of neurons makes our technique a more universal platform.

CONCLUSIONS

In summary, we demonstrated that the photothermal effect of GNRs localized on the plasma membrane

could be used to modulate neural activity. The suppression effect was highly reproducible and reversible and could also be sustained for long periods without cell damage. To our knowledge, this is the first report of a nanoparticle-based neuromodulation technique that can control neuronal activity through the mode of neural inhibition. Considering the potential need for neural suppression techniques in the treatment of complex brain disorders including epilepsy and Parkinson's disease, our nanotechnological approach represents a valuable tool for new applications in translational nanomedicine.

MATERIALS AND METHODS

Cell Culture. Hippocampal tissues were dissected from embryonic day 18 Sprague–Dawley rat brain. The tissues were rinsed with Hank's Balanced Salt Solution (HBSS, WelGENE, Korea), and they were triturated using a pipet tip in the HBSS solution, followed by centrifugation at 1000 rpm for 2 min. After the removal of supernatant, cells were seeded to poly-D-lysine (0.1 mg/mL in borate buffer, Sigma) coated microelectrode array (MEA, MultiCannel Systems) at the density of 800 cells/mm^2 and maintained in Neurobasal medium (Invitrogen) supplemented with B27 (2% v/v, Invitrogen), GlutaMAX (2 mM, Invitrogen), glutamate (12.5 μM, Sigma) and penicillin streptomycin (1% v/v, Invitrogen) in a humidified incubator with 5% CO_2 and 37 °C condition. After 3 days, half of the medium was changed without glutamate and was regularly changed every 5 days. The cultivation of cortex and olfactory bulb cells was carried out with the same protocol.

Gold Nanorod Preparation and Characterization. Gold nanorods (GNR) were synthesized by a seed mediated method as previously reported.[19] Briefly, 5 mL of 0.2 M Cetyltrimethylammonium bromide (CTAB, Sigma), 5 mL of 0.5 mM $HAuCl_4$ (Sigma), and 600 μL of 0.01 M $NaBH_4$ (Sigma) were mixed in ultrasonication bath. This seed solution was aged for 2 h. To grow the seed into rod shape, 12 μL of seed solution was mixed with 5 mL of 0.2 M CTAB, 5 mL of 1 mM $HAuCl_4$, 250 μL of 4 mM $AgNO_3$, and 70 μL of 78.84 mM ascorbic acid. The synthesized GNRs were washed by centrifuging at 10 000 rpm for 10 min and resuspended in ultrapure water. To coat the GNR surface with polyethylene glycol (PEG) molecules, 3 mg/mL of biterminal PEG (NH_2-PEG(5K)-SH or mPEG(5K)-SH, Nanocs) was reacted with 3 OD (optical density) of GNR solution for 2 h at room temperature. Free PEG molecules were removed by using dialysis kit (Thermo scientific). UV–vis absorption spectrum and zeta potential of GNRs were measured by SpectraMax Plus (Molecular devices) and Zetasizer Nano ZS (Malvern), respectively. Size and morphology of GNRs were observed by Tecnai G^2 F30 S-twin TEM instrument (operating at the accelerating voltage of 300 kV). Temperature change of the GNR solution during NIR irradiation was measured by IR thermographic camera (FLIR) and the acquired data was processed by MATLAB (Mathworks). Unless otherwise stated, NH_2-PEG-GNR was used in all experiments.

Cell Binding. Fluorescence molecules (Alexa Fluor 488 carboxylic acid, succinimidyl ester, Invitrogen) were conjugated to amine-terminated PEGylated GNRs to visualize GNR binding on the neuronal plasma membrane. Half of the amine groups on the GNR surface was used for conjugation of fluorescence molecules. Neurons were treated with 20 μg/mL of fluorescently tagged GNRs for 9 h and washed three times with PBS. Images were acquired using confocal microscopy (Leica) with 63× oil immersion lens (NA = 1.25).

Photothermal Stimulation. A fiber-optic laser (785 nm, 450 mW, B&W Tek) was used for a light source and the laser beam formed 5 mm diameter of illumination area on the MEA chip (Figure 2A). Hippocampal neuronal networks were cultured on a multichannel microelectrode array (MEA) chip and incubated with PEGylated GNRs for 9 h. The GNR-treated neurons were then repeatedly irradiated with a NIR laser (785 nm) at different incubation times without washing unbound GNRs in the medium. One cycle of photothermal stimulation was performed by turning on the NIR laser for 10 s followed by turning off the NIR laser for 20 s. This cycle was repeated 30 times in the spontaneous activity modulation tests. The repetitive laser switching was precisely controlled by TTL pulses. During the experiments, extracellular spikes of the neuronal network were recorded simultaneously from 59 microelectrodes of the MEA chip.

Neural Activity Recording. Neural recordings were obtained from neuronal cultures at the age of 11–18 DIV. Extracellular spikes from cultured neurons were sensed by 60-channels TiN microelectrode arrays (MultiChannel Systems, diameter 30 μm, electrode spacing 200 μm, 500 nm thickness of Si_3N_4 insulator). Electrode signals were amplified and digitized with an *in vitro* MEA system (Multichannel systems, gain 1100, bandwidth 10–8 kHz, sampling frequency 25 kHz). The recorded signals were filtered with a 200 Hz digital high pass filter (Butterworth, second order), and spikes were detected by setting the threshold level at six times the standard deviation of background noise in vendor provided software (MC Rack, MultiChannel Systems). Electrical stimulation was applied using an STG 2004 stimulator (MultiChannel Systems) at constant current stimulation mode. Cathodic-first biphaisc pulses were used with pulse width of 200 μs for each phase. Recording condition was maintained at 37 °C and 5% CO_2. Collected data were processed using NeuroExplorer (Nex technologies) and MATLAB (Mathworks). For drug response testing, bath application method was used. Briefly, drugs were mixed with 200 μL of media sampled from the cultured MEA chip. After 20 min of stabilization, the drug mixture was directly added onto the chip using a micropipette while neural spikes were being recorded. The final concentrations of drugs in the chip were set to be 10, 10 and 1 μM for AP5, CNQX, and fluoxetine, respectively.

Labeling Fluorescent Molecules to GNRs. Fluorescence molecules (Alexa Fluor 488 carboxylic acid, succinimidyl ester, Invitrogen) were conjugated to amine-terminated PEGylated GNRs to visualize GNR binding on the neuronal plasma membrane. First, optical density of the dye solution at a concentration of 8.3 μg/mL (in DI water) was measured by SpectraMax Plus (Molecular devices). And the number of the molecules were calculated by Beer–Lambert law: $A = a \times b \times c$, where A is the measured optical density, a is the molar absorptivity coefficient (L mol^{-1} cm^{-1}), b is cell length (cm) and c is concentration (mol/L). 10 μg/mL GNR solution was reacted with 8.3 μg/mL dye solution, for 1 h at room temperature. Free dyes were collected by using centrifugal filter (MWCO: 100 k, Millipore). The optical density of free dye solution was measured, and the change of the optical density was used to calculate the number of dyes conjugated to the GNRs. The total number of dye molecules bound per 1 μg GNRs was calculated to 4.172×10^{14}. On the basis of the calculation, fluorescence molecules were conjugated to the GNR surface to cover half of the amine groups.

Multiphoton Luminescence Imaging. The GNRs localized on the neural plasma membrane were visualized with a LSM 510 laser scanning microscope (10× water immersion lens, NA = 0.3, Zeiss) based on their intrinsic multiphoton luminescence (Figure S2, Supporting Information). A coherent chameleon pulsed NIR laser (800 nm) was used to excite the GNRs and the system collected emission light at the wavelengths ranged from 420 to 680 nm. Luminescence intensity of neurons was measured using ImageJ (NIH).

Cell Viability. Hippocampal neurons were cultured in 96 well black plates (Sigma) at the density of 800 cell/mm^2 for 14 DIV and treated with CTAB-coated GNRs or PEGylated GNRs at 1 and 10 μg/mL concentrations. After treatment for 24, 48, or 72 h, the cells were washed for 3 times with fresh medium. Calcein AM kit (Invitrogen) was used to quantify cell viability by measuring fluorescence intensity from live cells. The GNR-treated cells

were incubated with calcein AM dyes for 20 min and washed with phosphate buffer saline (PBS, pH 7.4, Invitrogen) for 3 times. Fluorescence intensity of the cells was measured by SpectraMax Gemini XPS (Molecular devices).

Immunostaining. Hippocampal neurons were fixed in ice cooling methanol for 5 min at −20 °C, and washed with PBS 3 times. The nonspecific binding of antibodies was blocked by 6% bovine serum albumin (BSA, Sigma) for 30 min, and washed with PBS 3 times. Primary antibodies (anti β-tubulin (1:500, Sigma), anti TREK-1 (1:200, Abcam)) that were diluted in 1.5% BSA were loaded to the cells for 24 h at 4 °C. After washing with PBS for 3 times, and secondary antibodies (Alexa Fluor 594 and 488 (1:200, Invitrogen)) that were diluted in 1.5% BSA were loaded for 1 h at 37 °C. After 3 times washing with PBS, Hoechst 33342 (1:200, Sigma) was loaded to cells for nucleus staining. After 10 min, cells were washed with PBS 3 times. Fluorescence images were taken by inverted microscopy (IX71, Olympus) with a 40× objective lens.

Data Analysis. Recording channels whose average firing rate was larger than 0.1 spikes/sec were selected as active channels and used for neural activity analysis. For the analysis of spontaneous activity, peri-event time histogram and raster plots were used with the NIR irradiation as an event. The change of spike rate (SR) with or without the NIR irradiation was calculated by the following equation: SR change (%) = $[SR_{(ON)} - SR_{(OFF)}]/SR_{(OFF)}$, where $SR_{(OFF)}$ and $SR_{(ON)}$ indicated the average spikes rate before and after the onset of NIR irradiation, respectively. $SR_{(ON)}$ covered the entire irradiation period (10 s) and $SR_{(OFF)}$ covered the 10 s window just before the onset of the irradiation. For the analysis of electrically evoked responses, spikes whose amplitude was greater than 45 μV were collected (Figure 3). Electrically evoked responses were quantified by counting the number of spikes in a poststimulus time window (window size: 100 ms) and estimating the instantaneous firing rate (Figure 3C) or the response probability based on the total number of trials (Figure 3E). As for the direct responses, spikes that appeared within 10 ms after the onset of electrical stimulation and the spikes with low jittering (standard deviation of response latency less than 5 ms) were only counted under the synapse blocking treatment (Figure 3D,E). The bin size of spike rate histogram during the drug experiments was 10 s (Figures 4 and 5). All statistics were performed with 1% of significant level ($\alpha = 0.01$).

Conflict of Interest: The authors declare no competing financial interest.

Acknowledgment. This research was supported by Basic Science Research Program through the National Research Foundation of Korea (NRF) funded by the Ministry of Science, ICT and Future Planning (NRF-2012R1A2A1A01007327, and NRF-2012R1A1A1011058).

Supporting Information Available: Supplementary methods and Figures S1−S11. This material is available free of charge *via* the Internet at http://pubs.acs.org.

REFERENCES AND NOTES

1. Dobson, J. Remote Control of Cellular Behaviour with Magnetic Nanoparticles. *Nat. Nanotechnol.* **2008**, *3*, 139–143.
2. Stanley, S. A.; Gagner, J. E.; Damanpour, S.; Yoshida, M.; Dordick, J. S.; Friedman, J. M. Radio-Wave Heating of Iron Oxide Nanoparticles can Regulate Plasma Glucose in Mice. *Science* **2012**, *336*, 604–608.
3. Huang, H.; Delikanli, S.; Zeng, H.; Ferkey, D. M.; Pralle, A. Remote Control of Ion Channels and Neurons through Magnetic-Field Heating of Nanoparticles. *Nat. Nanotechnol.* **2010**, *5*, 602–606.
4. Cho, M. H.; Lee, E. J.; Son, M.; Lee, J. H.; Yoo, D.; Kim, J. W.; Park, S. W.; Shin, J. S.; Cheon, J. A Magnetic Switch for the Control of Cell Death Signalling in *In Vitro* and *In Vivo* Systems. *Nat. Mater.* **2012**, *11*, 1038–1043.
5. Miyako, E.; Deguchi, T.; Nakajima, Y.; Yudasaka, M.; Hagihara, Y.; Horie, M.; Shichiri, M.; Higuchi, Y.; Yamashita, F.; Hashida, M.; *et al.* Photothermic Regulation of Gene Expression Triggered by Laser-Induced Carbon Nanohorns. *Proc. Natl. Acad. Sci. U. S. A.* **2012**, *109*, 7523–7528.
6. Wells, J. D.; Mahadevan-Jansen, A.; Kao, C. C.; Konrad, P. E.; Jansen, E. D. Transient Optical Nerve Stimulation: Concepts and Methodology of Pulsed Infrared Lase Stimulation of the Peripheral Nerve *In Vivo*. In *Neuroengineering*; DiLorenzo, D. J., Bronzino, J. D., Eds.; CRC Press: New York, 2008; pp 21-1−21-19.
7. Wells, J.; Kao, C.; Konrad, P.; Milner, T.; Kim, J.; Mahadevan-Jansen, A.; Jansen, E. D. Biophysical Mechanisms of Transient Optical Stimulation of Peripheral Nerve. *Biophys. J.* **2007**, *93*, 2567–2580.
8. Richter, C. P.; Matic, A. I.; Wells, J. D.; Jansen, E. D.; Walsh, J. T., Jr. Neural Stimulation with Optical Radiation. *Laser Photonics Rev.* **2011**, *5*, 68–80.
9. Shapiro, M. G.; Homma, K.; Villarreal, S.; Richter, C. P.; Bezanilla, F. Infrared Light Excites Cells by Changing Their Electrical Capacitance. *Nat. Commun.* **2012**, *3*, 736.
10. Liang, S.; Yang, F.; Zhou, C.; Wang, Y.; Li, S.; Sun, C. K.; Puglisi, J. L.; Bers, D.; Sun, C.; Zheng, J. Temperature-Dependent Activation of Neurons by Continuous Near-Infrared Laser. *Cell Biochem. Biophys.* **2009**, *53*, 33–42.
11. Boyden, E. S.; Zhang, F.; Bamberg, E.; Nagel, G.; Deisseroth, K. Millisecond-Timescale, Genetically Targeted Optical Control of Neural Activity. *Nat. Neurosci.* **2005**, *8*, 1263–1268.
12. Zhang, F.; Wang, L. P.; Brauner, M.; Liewald, J. F.; Kay, K.; Watzke, N.; Wood, P. G.; Bamberg, E.; Nagel, G.; Gottschalk, A.; *et al.* Multimodal Fast Optical Interrogation of Neural Circuitry. *Nature* **2007**, *446*, 633–639.
13. Williams, J. C.; Denison, T. From Optogenetic Technologies to Neuromodulation Therapies. *Sci. Transl. Med.* **2013**, *5*, 177ps6.
14. Chen, H.; Shao, L.; Li, Q.; Wang, J. Gold Nanorods and Their Plasmonic Properties. *Chem. Soc. Rev.* **2013**, *42*, 2679–724.
15. Park, J. H.; von Maltzahn, G.; Xu, M. J.; Fogal, V.; Kotamraju, V. R.; Ruoslahti, E.; Bhatia, S. N.; Sailor, M. J. Cooperative Nanomaterial System to Sensitize, Target, and Treat Tumors. *Proc. Natl. Acad. Sci. U. S. A.* **2010**, *107*, 981–986.
16. von Maltzahn, G.; Park, J. H.; Lin, K. Y.; Singh, N.; Schwoppe, C.; Mesters, R.; Berdel, W. E.; Ruoslahti, E.; Sailor, M. J.; Bhatia, S. N. Nanoparticles that Communicate *In Vivo* to Amplify Tumour Targeting. *Nat. Mater.* **2011**, *10*, 545–552.
17. Huang, X.; El-Sayed, I. H.; Qian, W.; El-Sayed, M. A. Cancer Cell Imaging and Photothermal Therapy in the Near-Infrared Region by Using Gold Nanorods. *J. Am. Chem. Soc.* **2006**, *128*, 2115–2120.
18. Kang, G.; Nam, Y. *In Vitro* Neuronal Activity Change Induced by Thermal Effects of Near-Infrared Laser Stimulation. *Proc. MEA Meet.* **2008**, *5*, 166–167.
19. Nikoobakht, B.; El-Sayed, M. A. Preparation and Growth Mechanism of Gold Nanorods (NRs) Using Seed-Mediated Growth Method. *Chem. Mater.* **2003**, *15*, 1957–1962.
20. Wang, H.; Huff, T. B.; Zweifel, D. A.; He, W.; Low, P. S.; Wei, A.; Cheng, J. X. *In Vitro* and *In Vivo* Two-Photon Luminescence Imaging of Single Gold Nanorods. *Proc. Natl. Acad. Sci. U. S. A.* **2005**, *102*, 15752–15756.
21. Goshen, I.; Brodsky, M.; Prakash, R.; Wallace, J.; Gradinaru, V.; Ramakrishnan, C.; Deisseroth, K. Dynamics of Retrieval Strategies for Remote Memories. *Cell* **2011**, *147*, 678–689.
22. Wagenaar, D. A.; Pine, J.; Potter, S. M. Effective Parameters for Stimulation of Dissociated Cultures Using Multi-Electrode Arrays. *J. Neurosci. Methods* **2004**, *138*, 27–37.
23. Steinlein, O. K. Genetic Mechanisms that Underlie Epilepsy. *Nat. Rev. Neurosci.* **2004**, *5*, 400–408.
24. Velíšek, L. Models of Chemically-Induced Acute Seizures. In *Models of Seizures and Epilepsy*; Pitkänen, A. P. A., Schwartzkroin, P. A., Moshé, S. L., Eds.; Elsevier Academic Press: Philadelphia, PA, 2006; pp 127−152.
25. Fisher, R. S. Animal Models of the Epilepsies. *Brain Res. Rev.* **1989**, *14*, 245–278.
26. Honore, E. The Neuronal Background K2P Channels: Focus on TREK1. *Nat. Rev. Neurosci.* **2007**, *8*, 251–261.
27. Hervieu, G. J.; Cluderay, J. E.; Gray, C. W.; Green, P. J.; Ranson, J. L.; Randall, A. D.; Meadows, H. J. Distribution and Expression of TREK-1, a Two-Pore-Domain Potassium Channel, in the Adult Rat CNS. *J. Neurosci.* **2001**, *103*, 899–919.

28. de la Pena, E.; Malkia, A.; Vara, H.; Caires, R.; Ballesta, J. J.; Belmonte, C.; Viana, F. The Influence of Cold Temperature on Cellular Excitability of Hippocampal Networks. *PLoS One* **2012**, *7*, e52475.
29. Kennard, L. E.; Chumbley, J. R.; Ranatunga, K. M.; Armstrong, S. J.; Veale, E. L.; Mathie, A. Inhibition of the Human Two-Pore Domain Potassium Channel, TREK-1, by Fluoxetine and Its Metabolite Norfluoxetine. *Br. J. Pharmacol.* **2005**, *144*, 821–829.
30. Heurteaux, C.; Lucas, G.; Guy, N.; El Yacoubi, M.; Thummler, S.; Peng, X. D.; Noble, F.; Blondeau, N.; Widmann, C.; Borsotto, M.; *et al.* Deletion of the Background Potassium Channel TREK-1 Results in a Depression-Resistant Phenotype. *Nat. Neurosci.* **2006**, *9*, 1134–1141.
31. Paz, J. T.; Davidson, T. J.; Frechette, E. S.; Delord, B.; Parada, I.; Peng, K.; Deisseroth, K.; Huguenard, J. R. Closed-Loop Optogenetic Control of Thalamus as a Tool for Interrupting Seizures after Cortical Injury. *Nat. Neurosci.* **2013**, *16*, 64–70.
32. Tonnesen, J.; Sorensen, A. T.; Deisseroth, K.; Lundberg, C.; Kokaia, M. Optogenetic Control of Epileptiform Activity. *Proc. Natl. Acad. Sci. U. S. A.* **2009**, *106*, 12162–12167.
33. Duke, A. R.; Jenkins, M. W.; Lu, H.; McManus, J. M.; Chiel, H. J.; Jansen, E. D. Transient and Selective Suppression of Neural Activity with Infrared Light. *Sci. Rep.* **2013**, *3*, 2600.
34. Medhurst, A. D.; Rennie, G.; Chapman, C. G.; Meadows, H.; Duckworth, M. D.; Kelsell, R. E.; Gloger, I. I.; Pangalos, M. N. Distribution Analysis of Human Two Pore Domain Potassium Channels in Tissues of the Central Nervous System and Periphery. *Mol. Brain Res.* **2001**, *86*, 101–114.